



OPEN

A novel variant in *TLE6* is associated with embryonic developmental arrest (EDA) in familial female infertility

Mojdeh Akbari^{1,7}, Mehdi Mohebi^{2,7}, Katayon Berjis³, Amin Ghahremani^{4,5},
 Mohammad Hossein Modarressi^{1✉} & Soudeh Ghafouri-Fard^{2,6✉}

This study aims to identify genetic causes of familial female infertility characterized by embryonic developmental arrest (EDA) and repeated implantation failure (RIF) with oocyte donation IVF cycle. We used Whole-exome sequencing and Sanger validation to find causative genes in an Iranian consanguineous family that had 3 infertile daughters, 4 fertile daughters, and 2 fertile sons. All patients in this consanguineous family exhibited typical manifestations of unexplained RIF and EDA. Genetic analysis identified a homozygous missense variant (c.G1054C:p.G352R) in exon 13 of the *TLE6* gene that cosegregated with the EDA phenotype in an autosomal recessive pattern. Other members of the family, the gene carriers, remain clinically asymptomatic and fertile. Our findings identify a novel nonsynonymous variant, c.G1054C:p.G352R, in the *TLE6* gene within a consanguineous Iranian family with autosomal-recessive female infertility and broaden the genetic spectrum of *TLE6*-associated EDA.

Infertility is a common health problem defined as failure to conceive after one year of regular unprotected sexual intercourse. It is a notable reproductive health problem that affects more than 10% of people of reproductive age^{1–3}. The technique of in vitro fertilization (IVF) is considered as a solution for a large number of infertile couples. Embryonic developmental arrest (EDA) is one of the several factors that can limit the success rate of this technique and is responsible for the high number of embryos that arrest during the first week of in vitro development. Approximately 10–15% of IVF embryos arrest in mitosis at the 2- to 4-cell cleavage stage and show no signs of cell death. Accumulating evidence indicates that this is a common phenomenon in humans. Approximately 10% of all human embryos created by IVF or intracytoplasmic sperm injection become permanently arrested in the early stages of cleavage in culture, and 40% of patients have at least one arrested embryo per treatment cycle⁴. The permanent arrest of embryos is a non-apoptotic event, since no morphological, no biochemical, and no molecular evidence of apoptosis has been observed before the 8-cell stage in bovine and human embryos^{5–8}. Since the evaluation of the phenotype associated with EDA in any situation except recurrent IVF failure (RIF) is difficult and accessibility to it in the natural environment is not possible, the genetic cause of EDA in humans is not fully understood. According to previous studies, we can point to chromosomal abnormalities, and single-gene mutations in some genes such as *NLRP2*⁹, *NLRP5*⁹, *FBXO43*¹⁰, *PADI6*¹¹, *Btg4*¹², *CDC20*¹³, *MOS*^{14,15}, and *ACTL7A*¹⁶ as the genetic causes of EDA. This process is also associated with aberrant regulation of several signaling pathways such as the Wnt and TGF β signaling pathways¹⁷. In the stage of oocyte maturation, oocytes accumulate an essential amount of maternal RNAs and proteins that are used by the early embryo to zygotic genome activation (ZGA)^{18,19}. Maternal factors regulate transcription, both directly and indirectly during ZGA¹⁸. Studies in mouse introduced *TLE6* as a fundamental maternal effect gene in embryonic preimplantation development^{20,21}. It seems that *TLE6* has a pivotal role in symmetric cell division at the 2-cell stage. It stabilized

¹Department of Medical Genetics, School of Medicine, Tehran University of Medical Sciences, Tehran, Iran. ²Department of Medical Genetics, School of Medicine, Shahid Beheshti University of Medical Sciences, Tehran, Iran. ³Department of Reproductive Biology, The Academic Center for Education, Culture and Research, Qom Branch, Qom, Iran. ⁴Pars Human Gene Company, Tehran, Iran. ⁵Department of Electrical Engineering, Sharif University of Technology, Tehran, Iran. ⁶Urogenital Stem Cell Research Center, Shahid Beheshti University of Medical Sciences, Tehran, Iran. ⁷These authors contributed equally: Mojdeh Akbari and Mehdi Mohebi. ✉email: modaresi@tums.ac.ir; s.ghafourifard@sbmu.ac.ir

the subcortical maternal complex (SCMC) which controls symmetric cell division in zygotes^{22,23}. *TLE6*-null embryos have died at the cleavage stage^{21,22}.

WD40-Repeat Proteins (WDR proteins) are one of the largest families encoded by humans²⁴. They play important roles in many fundamental biological processes such as apoptosis²⁵, DNA damage response²⁶, protein degradation²⁷, RNA processing²⁸, transcription regulation^{29,30}, histone modification³¹, and signal transduction³². WDR proteins often act as scaffolds to engage other molecules, forming protein–protein interactions or functional complexes²⁴. They are classified broadly into 21 classes based on their domain architectures²⁴. Transducin-like enhancer protein (TLE) family belongs to class 7 (TLE_N + WD40)^{24,33}. One such WDR protein, TLE6, belongs to a TLE family that perform numerous critical functions such as controlling and regulating cell cycle progression, gene expression, post-translational modifications, and developmental process³³. TLE6 has also been shown as a critical protein required in the embryonic process for female pregnancy. variants in the *TLE6* gene at the 19p13.3 locus (OMIM *612399) are responsible for autosomal recessive preimplantation embryonic lethality and EDA. To date, 13 variants have been identified^{34–40}. The phenotypic spectrum seen in *TLE6* mutated patients in these reports suggested sex-associated and genotype–phenotype correlations. Females with bi-allelic variant that result in complete loss of TLE6 active site function exhibit infertility. In contrast, males and females with mono-allelic variant are fertile.

In this study, we characterized the phenotypic spectrum in a consanguineous Iranian family with autosomal recessive EDA due to variant in the *TLE6* gene. Here, we report three Iranian infertile sisters due to variant in *TLE6*. In-depth phenotyping of all members in this consanguineous family pinpoints a clear genotype–phenotype correlation between *TLE6* and EDA. We also report a novel variant [NM_001143986(*TLE6*): c. 1054 G>C (p. G352R)].

Material and methods

Subjects. One Iranian family segregating apparent RIF and EDA was ascertained for this study. Affected individuals underwent clinical examination. Whole blood samples were collected from all family members and genomic DNA was extracted, after obtaining written informed consent. This protocol has been approved by the ethics committee of the Shahid Beheshti and Tehran Universities of Medical Science, Tehran, Iran.

Next-generation sequencing (NGS). WES (Whole Exome Sequencing) for the family was performed, using the SureSelect XT V6 Human All Exon kit (Agilent Technologies, Santa Clara, CA, USA) following the manufacturer's protocol. After library quantification and pooling, samples were sequenced on an Illumina Next-Seq 500 System (Illumina, San Diego, CA, USA) using the Illumina V3 High Throughput kit. For 3 people in the family (II.11, II.16, II.18) library preparation, sequencing, and bioinformatics analysis were performed using illumina Platform.

Segregation analysis. Segregation analysis was completed by Sanger sequencing on an ABI 3130 Sequencer (Foster City, CA, USA). All sequencing chromatograms were compared to published cDNA sequences for *TLE6* (NM_001143986.1), and nucleotide changes were detected using Finch TV Aligner.

Ethics approval and consent to participant. All procedures performed in studies involving human participants were in accordance with the ethical standards of the institutional and/or national research committee and with the 1964 Helsinki declaration and its later amendments or comparable ethical standards. Informed consent forms were obtained from all study participants. The study protocol was approved by the ethical committee of Shahid Beheshti University of Medical Sciences and Tehran University of Medical Sciences. All methods were performed in accordance with the relevant guidelines and regulations.

Result

Bioinformatics analysis. Data quality was determined by FASTQC. Paired-end sequences were mapped to the human genome (UCSC hg19) using Burrows-Wheeler Aligner (BWA). Functional variant detection and annotation of genetic variants from high-throughput sequencing data were performed with the GATK (Genome Analysis Toolkit) and ANNOVAR software, respectively. Additionally, variants were filtered with MAF (minor allele frequencies) from the dbSNP, hapmap, Mutation Taster, Intervar, OMIM, Kaviar, 1000 Genomes, gnomAD, ExAC, and the Iranome. First, we filtered variants for quality (depth > 10 and quality score > 30) which was followed by minor allele frequency (MAF) (< 2%). Then, variants were prioritized based on variant-type (missense, nonsense, indel, or splice site), followed by *in-silico* prediction for conservation (GERP and PhyloP), and predicted deleteriousness (SIFT, PolyPhen2, and the CADD).

For extracting the candidate variants from genomic data of the affected (II.11, II.18) and their healthy sibling (II.16) we consider two hypotheses about infertility and embryonic developmental arrest (EDA) patients.

1. Variants that are associated with dominant diseases:

All heterozygous variants are present in the patients and absent in the healthy controls.

2. Variants that are associated with recessive diseases:

Homozygous variants are present in the patients and heterozygous or absent in the healthy controls.
Compound heterozygous variants existing in the patients and missing in the healthy controls.

Patient	Age years	Age of marriage	Duration of infertility years	IUI	IVF/ICSI attempts with her oocyte	Outcomes	Total no. of PB1 oocytes retrieved	No. of fertilized oocytes	Viable embryos on day 3	IVF/ICSI attempts with oocyte donation	Outcomes after 2 embryo transfer in each time	Spouse information (Semen analysis)
II.3	56	17	31	3	3	All the embryos were arrested on day 3	1st.4	1st.2	0	0	0	Not available (But he got married and has 2 children)
							2st.5	2st.2	0			
							3st.9	3st.0	0			
II.11	37	21	15	1	3	All the embryos were arrested on day 3	1st.5	1st.3	0	3	1st. – 2st. – 3st.+	Sperm count: 88 Motility: 81.4% Morphology: 6% DFI TUNEL: 7% SCSA: 11%
							2st.5	2st.4	0			
							3st.4	3st.0	0			
II.18	32	21	10	1	3	All the embryos were arrested on day 3	1st.7	1st.2	0	3	1st. – 2st.– 3st.+	Sperm count: 97 Motility: 65% Morphology: 2% DFI: TUNEL: 4% SCSA: 10%
							2st.7	2st.0	0			
							3st.5	3st.0	0			

Table 1. Oocyte and embryo characteristics of the IVF and ICSI attempts of the female patients.

$$\text{Selected Variants} = \bigcap_{i=1}^2 \text{Patients}(i) - \bigcup_{i=1}^1 \text{Healthy}(i)$$

By using this pattern, we found 7 variants in 7 genes (*WFS1*, *PLA2G7*, *IL17F*, *CHD4*, *A2ML1*, *CHRNA4*, *TLE6*). Six of them were placed in the first hypothesis, which we could not find any association for them with infertility and EDA, and one of them (*TLE6*) was placed in the second hypothesis, we found it in the homozygous format in the affected and heterozygous format in their healthy sister.

Clinical characteristics of the patients. The clinical information of the three patients carrying the biallelic *TLE6* variants are listed in Table 1, and their family pedigrees are shown in Fig. 1.

All assessments including karyotypes, menstrual cycle assays, sex hormone levels, and transvaginal sonography revealed no abnormalities. Furthermore, their husbands also showed normal karyotypes and normal semen parameters (sperm morphology, motility, and sperm concentration) (Table 1). This Iranian consanguine family raised seven daughters. Three of them (II-3, II-11, and II-18) had infertility for several years. All the affected individuals underwent several IVF attempts. Two of the affected sisters (II-11 and II-18) even underwent three oocyte donation IVF attempts in the Reproductive Medicine Center.

The II-3 patients (56 years old) had undergone 3 unsuccessful IUI and 3 IVF/ICSI attempts. Totally 18 MII oocytes were retrieved in the three attempts. Only four oocytes were normally fertilized with two pronuclei (PN) zygotes, while the others were abnormally fertilized with 0PN or degradation on day 1. After cultivation, most of her embryos were arrested at the early stages with heavy fragmentation, and only two poor-quality embryos were available for transfer. Although the patient underwent 2 embryo transfer cycles, she failed to obtain a successful pregnancy. Her spouse got married and now has 2 children.

The other affected sister (II-11, 37 years old) underwent 1 unsuccessful IUI and 3 IVF/ICSI attempts with her oocytes and 3 IVF/ICSI attempts with donated oocytes. A total of 14 MII oocytes were retrieved in the 3 attempts. Some of her oocytes were abnormally fertilized with 0PN; 7 of them showed normal fertilization with 2PN zygotes on day 1. All of her embryos were arrested at the early stages having heavy fragmentation. Finally, after hysteroscopy and IVF with oocyte donation she got pregnant. In 3 IVF attempts with donated oocyte, 2 first attempts were failed and finally, in the last one, she got pregnant. Before the 3rd attempt, diagnostic hysteroscopy was performed on her and everything was normal. Her spouse's information is available on the Table 1.

The proband (II-18, 32 years old) underwent 1 unsuccessful IUI, 3 IVF/ICSI attempts with her oocytes, and 3 IVF/ICSI attempts with donated oocytes. A total of 19 MII oocytes were retrieved in the three attempts. Only 2 oocytes were normally fertilized with two pronuclei (PN) zygotes, while the others were abnormally fertilized with 0PN or degradation on day 1. After cultivation, all of her embryos were arrested at the early stages with heavy fragmentation. Totally, in 3 IVF attempts with donated oocyte, 2 first attempts were failed and finally, in the last one, she got pregnant. Before the 3rd attempt, diagnostic hysteroscopy was performed on her and everything was normal. Her spouse's information is available in the Table 1 and is completely normal.

Identification of novel variant in *TLE6*. All patients in this consanguineous family exhibited typical manifestations of unexplained RIF and EDA. Genetic analysis identified a homozygous missense variant

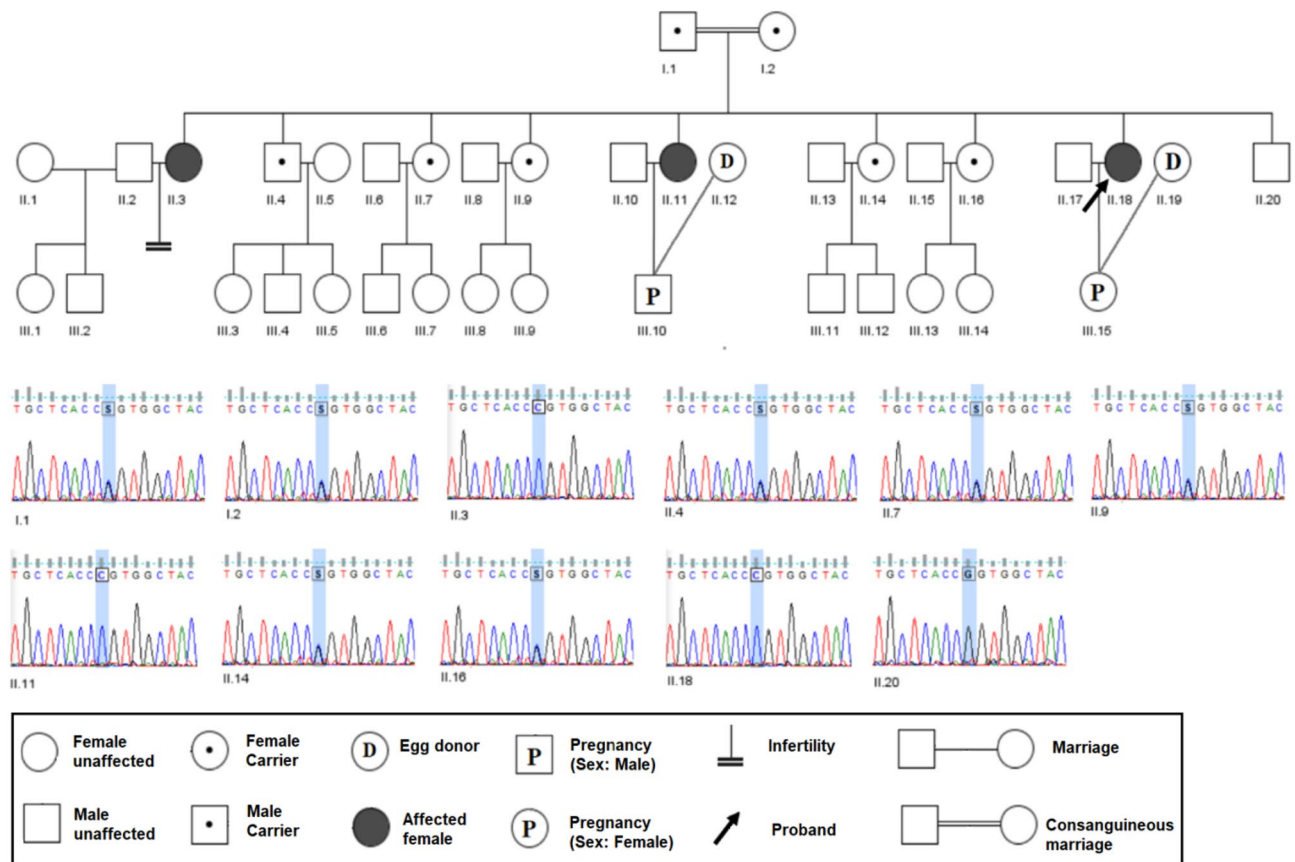


Figure 1. Pedigree of the studied family. Identification of *TLE6* variant in affected individuals and other family members. (*TLE6*: NM_001143986: exon13: c. G1054C: p. G352R).

(c.G1054C:p.G352R) in exon 13 of the *TLE6* gene that cosegregated with the EDA phenotype in an autosomal recessive pattern (NCBI, ClinVar accession number is SCV002525878.). Other members of the family, gene carriers, remain clinically asymptomatic and fertile.

The homozygous variant [NM_001143986(*TLE6*): c.1054G>C (p. G352R)] was identified in the proband and all of her affected sisters. This variant was verified by Sanger sequencing. Both of the parents, four fertile elder sisters, and one elder brother were heterozygous carriers, indicating a recessive inheritance pattern (Fig. 1). This variant has not been reported in ClinVar, HGMD, gnomAD, Iranome, ExAC, dbSNP, and 1000G. Based on this situation this is a novel variant (Tables 2 and 3).

Results of conservative and in silico analysis. The amino acids at position p.G352 of *TLE6* were highly conserved in 141 different taxonomies, suggesting that the variant was likely pathogenic. The location of the *TLE6* variant and the conservation analysis among different species are shown in Fig. 2. The variant identified in this study (c.G1054C:p.G352R) resides in the buried residue of the WDR2 domain and seems to play a central role in the enzyme activity (Fig. 3). According to the three-dimensional (3D) structure of *TLE6*, the nonsynonymous variant caused a replacement of glycine with arginine at position 352, leading to the production of 30 new binding sites and deactivation of all of its active sites and 20 native binding sites compared with the Wild type (Fig. 3).

By using I-Taster, we found that *TLE6* has 3 active site residues and 33 binding site residues. G352R variant gives rise to loss of all of its active site residues and 20 native binding site residues and achievement of 30 new binding sites, as a result, this variant caused *TLE6* to have no active site and 43 binding sites (For more detail refer to attachments).

Phenotypic spectrum of the patients with *TLE6* variant p.G352R. We used light microscopy to observe the development and morphology of the embryos from family members II-5 and II-8 for 5 consecutive days in their last ICSI attempt. Five of the embryos on day 3 were arrested, whereas the others had a high percentage of fragmentation, and all of them failed to form blastocysts (Fig. 4).

The morphology of the embryo is derived from the control and the proband, respectively.

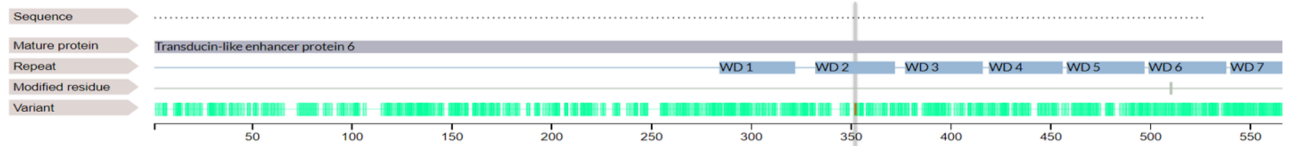
Variant allele	Homozygous
NM and location	TLE6:NM_024760:exon12:c.G685C:p.G229R, TLE6:NM_001143986:exon13:c.G1054C:p.G352R
start	2989593
cDNA alteration	c.G1054C
Protein alteration	p.G352R
Variant type	nonsynonymous SNV
ExAC (all/Asian)	Not found
gnomAD (all/Asian)	Not found
Iranome	Not found
SIFT	Damage
PolyPhen-2	Damage
Mutation taster	Damage
CADD-phred	25.2
varsome	VUS (PM2, PP3)
InterVar	VUS
Fraklin	VUS (PM2)
ClinVar	N/A
Hom f	N/A
AF	N/A
CADD	23.3
DANN	0.9977
Aggregated prediction	Uncertain

Table 2. Characteristics of the identified variant in the current study.

	Variant	Exon/intron	Inheritance	year	Ref	NCBI number
1	c.1529C>A (p.S510Y)	No data	Homozygous	2015	Alazami ⁴⁰	VCV000222026.2
2	c.1133delC, (p.A378Efs*75)	No data	Homozygous	2018	Xueqian Wang ³⁹	VCV000453260.1
3	c.1226G>A (p.Arg409Gln)	Exon 13	Homozygous	2020	Jing Lin ³⁸	Not available
4	c.1621G>A (p.Glu541Lys)	Exon 17	Homozygous	2020	Jing Lin ³⁸	Not available
5	c.388G>A (p.Asp130Asn)	Exon 7	Compound heterozygous	2020	Jing Lin ³⁸	Not available
6	c.1507G>A (p.Val503Ile)	Exon 15	Compound heterozygous	2020	Jing Lin ³⁸	Not available
7	c.541 + 1G>A	Intron7	Homozygous	2021	Bin Mao ³⁴	Not available
8	c.1245 – 2 A>G	Intron13	Homozygous	2021	Juan Liu ³⁵	Not available
9	c.1631_1632delCA (p.Pro544Argfs*5)	Exon 17	Homozygous	2021	Manyu Zhang ⁴¹	Not available
10	c.475_476delCT, (p.Leu159Aspfs*14)	Exon 7	Homozygous	2021	Manyu Zhang ⁴¹	Not available
11	c.222G>C, (p.Gln74His)	Exon 5	Compound heterozygous	2021/2021	Manyu Zhang ⁴¹ /Wei Zheng ³⁷	Not available
12	c.798_799insG, (p.Gln267Alafs*54)	Exon 12	Compound heterozygous	2021	Manyu Zhang ⁴¹	Not available
13	c.893C>G, (p.Thr298Arg)	Exon 13	Homozygous	2021	Wei Zheng ³⁷	Not available
14	c.719C>G (p.Ala240Gly0)	Exon 12	Homozygous and Compound heterozygous	2021	Wei Zheng ³⁷	Not available
15	c.1564G>C (p.Asp522His)	Exon 17	Homozygous	2021	Wei Zheng ³⁷	Not available
16	c.1013 G>A (p.Arg338His)	Exon14	Homozygous and Compound heterozygous	2021	Wei Zheng ³⁷	Not available
17	c.1337G>A (p.Trp446*)	Exon 17	Homozygous and Compound heterozygous	2021	Wei Zheng ³⁷	Not available
18	c.1054 G>C (p.G352R)		Homozygous	2022	Our study	Not available

Table 3. Overview of *TLE6* variants described in EDA.

A.



B.

Homo sapiens	LRTCLLSNSRSLLTGGYNL-Lynx canadensis	LRTCLLSSDSTLLAGGHNL-Callorhinus ursinus	LRTCLLAPTSTLLTGGHNL-
Mus musculus	LRTCLLSNSRSLTFAGGYNL-Rhinopithecus bieti	LRTCLLSNSRSLLTGGYNL-Eumetopias jubatus	LRTCLLAPTSTLLTGGHNL-
Rattus norvegicus	LRTCLLSNSRSLTFAGGYNL-Rhinopithecus roxellana	LRTCLLSNSRSLTFAGGHSL-Mastomys coucha	LRTCLLSNSRSLTFAGGSNL-
Bos taurus	LRTCLLFSNSTLLTGGHNL-Nomascus leucogenys	LRTCLLSNSRSLETFGGYNL-Suricata suricatta	LRTCLLADSTLLTGGHNL-
Pan troglodytes	LRTCLLSNSRSLLTGGYNL-Bos mutus	LRTCLLFSNSTLLTGGHNL-Aotus nancymaae	LRTCLLSNSRSLLAGGYNL-
Canis lupus familiaris	LRTCLLSSDSTLLTGGHNL-Panthera tigris	LRTCLLSSDSTLLAGGHNL-Onychomys torridus	LRTCLLSSNSRSLTFAGGHNL-
Ovis aries	LRTCLLFSNSTLLTGGHNL-Lontra canadensis	LRTCLLSPSTLLTGGHNL-Monodon monoceros	LRTCLLFSNSTALLTGGHNL-
Macaca mulatta	LRTCLLSNSRSLLTGGYNL-Microtus ochrogaster	LRTCLLSNSRSLTFAGGHSL-Phocoena sinus	LRTCLLFSNSTALLTGGHNL-
Equus caballus	LRTCLLFSNSTLLTGGHNL-Hylobates moloch	LRTCLLSNSRSLETFGGYNL-Ictidomys tridecemlineatus	LRTCLLFSNSTLLTGGHNL-
Mesocricetus auratus	LRTCLLSNSRSLTFAGGHNL-Bubalus bubalis	LRTCLLFSNSTLLTGGHNL-Bison bison	LRTCLLFSNSTLLTGGHNL-
Nannospalax galii	LRTCLLSPDRSLTFAGGQNL-Phyllostomus discolor	LRTCLLFSNSTALLTGGHNL-Talpa occidentalis	LRTCLLSPNSMTLLVGGNSL-
Dasyypus novemcinctus	LRTCLLCPDGAALLTGGGRL-Lagenorhynchus obliquidens	LRTCLLFSNSTALLTGGHNL-Jaculus jaculus	LRTCLLSSDSTLLAGGHNL-
Erinaceus europaeus	LHSCLLSPDSSLVGGDSL-Marmota flaviventris	LRTCLLSNSRSLTFAGGHNL-Castor canadensis	LRTCLLSSDSTLLAGGHNL-
Pteropus alecto	LRTCLLFSNSTLLTGGHNL-Hyaena hyaena	LRTCLLSPDSTLLTGGHNL-Trachypithecus francoisi	LRTCLLSSDSTLLAGGHNL-
Rousettus aegyptiacus	LRTCLLFSNSTLLTGGHNL-Dipodomys spectabilis	LRTCLLFSNSTLLTGGHNL-Myotis lucifugus	LRTCLLSSDSTLLAGGHNL-
Artibeus jamaicensis	LRTCLLFPNSTALLTGGHNL-Myotis brandtii	LRTCLLFSNSTLLTGGHNL-Rhinolophus ferrumequinum	LRTCLVSSDSTLLTGGHNL-
Desmodus rotundus	LRTCLLFPNSTALLTGGHNL-Microtus oregoni	LRTCLLFSNSTLLTGGHNL-Oryx dammah	LRTCLLFSNSTLLTGGHNL-
Sapajus apella	LRTCLLSNSRSLLAGGYNL-Ursus arctos horribilis	LRTCLLSPSTLLTGGHNL-Chlorocebus sabaeus	LRTCLLFSNSTLLTGGHNL-
Cercocebus atys	LRTCLLSNSRSLLTGGYNL-Lipotes vexillifer	LRTCLLFSNSTALLTGGHNL-Arvicanthis niloticus	LRTCLVSSNSRSLTFAGGYNL-
Meriones unguiculatus	LRTCLLSTNSRSLFAGGHNL-Macaca fascicularis	LRTCLLSNSRSLLTGGYNL-Orcinus orca	LRTCLLFSNSTALLTGGHNL-
Mus caroli	LCTCLLSNSRSLTFAGGYNL-Macaca nemestrina	LRTCLLSNSRSLLTGGYNL-Tursiops truncatus	LRTCLLFSNSTALLTGGHNL-
Mus pahari	LRTCLLSNSRSLTFAGGQNL-Papio anubis	LRTCLLSNSRSLLTGGYNL-Delphinapterus leucas	LRTCLLFSNSTALLTGGHNL-
Rattus rattus	LRTCLLSNSRSLTFAGGYNL-Theropithecus gelada	LRTCLLSNSRSLLTGGYNL-Physeter catodon	LRTCLLFSNSTALLTGGHNL-
Cavia porcellus	LRACLLAPDGSRLFAGGHNL-Mandrillus leucophaeus	LRTCLLSNSRSLETFGGYNL-Balaenoptera musculus	LRTCLLFSNSTALLTGGHNL-
Ocotodon degus	LRTCLLTPNGSMLLAGGHNL-Gorilla gorilla gorilla	LRTCLLSNSRSLLTGGYNL-Loxodonta africana	LRTCLLFPDSTALLTGGSNL-
Heterocephalus glaber	LRTCLLFPNGKVLLAGGHNL-Pan paniscus	LRTCLLSNSRSLLTGGYNL-Equus asinus	LRTCLLFSNSTLLTGGHNL-
Molossus molossus	LRTCLLFSNSTLLTGGYNL-Pongo abelii	LRTCLLSNSRSLLTGGYNL-Equus przewalskii	LRTCLLFSNSTLLTGGHNL-
Choloepus didactylus	LRTCLLFPDSTLLAGGSSL-Vulpes vulpes	LRTCLLSSDSTLLTGGHNL-Sus scrofa	LRTCLLMSNSTLLTGGHNL-
Saimiri boliviensis boliviensis	LRTCLLSNSRSLLAGGYNL-Ailuropoda melanoleuca	LCTCLLSPSTLLTGGHNL-Camelus bactrianus	LRTCLLFSNSTALLTGGHNL-
Ursus maritimus	LRTCLLSPSTLLTGGHNL-Felis catus	LRTCLLSSDSTLLAGGHNL-Camelus dromedarius	LRTCLLFSNSTALLTGGHNL-
Eptesicus fuscus	LRTCLLFSNSTLLTGGHNL-Panthera pardus	LRTCLLSSDSTLLAGGHNL-Odocoileus virginianus texanus	LRTCLLFSNSTALLTGGHNL-
Neomonachus schauinslandi	LRTCLLAPTSTLLTGGHNL-Puma concolor	LRTCLLSSDSTLLAGGHNL-Bos indicus	LRTCLLFSNSTLLTGGHNL-
Bos indicus x Bos taurus	LRTCLLFSNSTLLTGGHNL-Zalophus californianus	LRTCLLAPTSTLLTGGHNL-Capra hircus	LRTCLLFSNSTLLTGGHNL-
Vicugna pacos	LRTCLLFSNSTALLTGGHNL-Odobenus rosmarus divergens	LRTCLLAPTSTLLTGGHNL-Ochotona princeps	LRTCLLFSNSTLLTGGHNL-
Microcebus murinus	LRTCLLSANSRSLTFGGYNL-Halichoerus grypus	LRTCLLAPTSTLLTGGHNL-Urocyon parryi	LRTCLLFSNSTLLTGGHNL-
Otolemur garnettii	LRTCLLSNSRSLTFGGYNL-Leptonychotes weddellii	LRTCLLAPTSTLLTGGHNL-Dipodomys ordii	LRTCLLADSNSTLLAGGHNL-
Acinonyx jubatus	LRTCLLSSDSTLLAGGHNL-Phoca vitulina	LRTCLLAPTSTLLTGGHNL-Cricetulus griseus	LRTCLLSSNSKTLFAGGHNL-
Chinchilla lanigera	LRTCLLAPNGRTLTFAGGHNL-Globicephala melas	LRTCLLFSNSTALLTGGHNL-Peromyscus leucopus	LRTCLLFSNSTLLTGGHNL-
Nipponia nippon	IRSCKLLPDGRSLIVGGE-A-Piliocolobus tephrosceles	LRTCLLSNSRSLLTGGYNL-	LRTCLLFSNSTLLTGGHNL-
Ochotona curzoniae	LRTCLLTSNNRSLLAGGHSL-Fukomya damarensis	LRTCLLAPNGKMLFAGGHNL-	LRTCLLFSNSTLLTGGHNL-
Pteropus vampyrus	LRTCLLFSNSTLLTGGHNL-Arvicola amphibius	LRTCLLFSNSTLETFGGHNL-	LRTCLLFSNSTLLTGGHNL-
Pteropus giganteus	LRTCLLFSNSTLLTGGHNL-Puma yagouaroundi	LRTCLLSSDSTLLAGGHNL-	LRTCLLFSNSTLLTGGHNL-
Manis pentadactyla	LHACLSSDGGTPLSGSHGL-Neophocaena asiaeorientalis asiaeorientalis	LRTCLLFSNSTALLTGGHNL-	LRTCLLFSNSTLLTGGHNL-
Condylura cristata	LRTCLLTPSMTLLMGNSL-Cebus imitator	LRTCLLFSNSRSLTFAGGYNL-	LRTCLLFSNSTLLTGGHNL-
Hipposideros armiger	LRTCLVSSDSTLLTGGHNL-Ceratotherium simum simum	LRTCLLFSNSTLLTGGHNL-	LRTCLLFSNSTLLTGGHNL-
Myotis davidii	LRTCLLFPNSTALLTGGHNL-Trichechus manatus latirostris	LRTCLLFPDSTALLTGGSNL-	LRTCLLFSNSTLLTGGHNL-
Peromyscus maniculatus bairdii	LRTCLLFSNSTLLTGGHNL-		
Canis lupus dingo	LRTCLLSSDSTLLTGGHNL-		
Miniapterus natalensis	LRTCLLFSNSTLLTGGHNL-		
Balaenoptera acutorostrata scammoni	LRTCLLFSNSTALLTGGHNL-		
Colobus angolensis palliatus	LRACLLSSNSRSLLTGGYNL-		
Propithecus coquerelli	LRACLLSSNSRSLTFAGGHNL-		
Camelus ferus	LRTCLLFSNSTALLTGGHNL-		
Galeopterus variegatus	LRTCLLSSDSTLLTGGHNL-		
Gramomys surdaster	LRTCLLFSNSRSLTFAGGYNL-		
Vulpes lagopus	LRTCLLSSDSTLLTGGHNL-		

Figure 2. The locations and conservation of mutated residues in *TLE6* (*TLE6*:NM_001143986:exon13:c.G1054C:p.G352R). (A) The position of the variant is indicated in the genomic structure and protein structure of *TLE6*. (B) Conservation of mutated amino acids in *TLE6* among 141 different taxonomies. The residue G352 is highly conserved across species.

Discussion

Many infertile couples have experienced recurrent IVF/ICSI failed attempts. In some of them, the obtained oocytes and ovulatory status look normal, but zygote formation and embryonic development are severely impaired. This study aims to identify genetic causes of familial female infertility characterized by EDA and RIF. We used whole-exome sequencing and Sanger validation to find causative genes in an Iranian consanguineous family that has 9 children, 3 infertile daughters, 4 fertile daughters, and 2 fertile sons. All patients in this consanguineous family exhibited typical manifestations of unexplained RIF and EDA. Genetic analysis identified a novel homozygous missense variant (c.G1054C:p.G352R) in exon 13 of the *TLE6* gene that segregated with the EDA phenotype in an autosomal recessive pattern. Other members of the family, gene carriers, remain clinically asymptomatic and fertile.

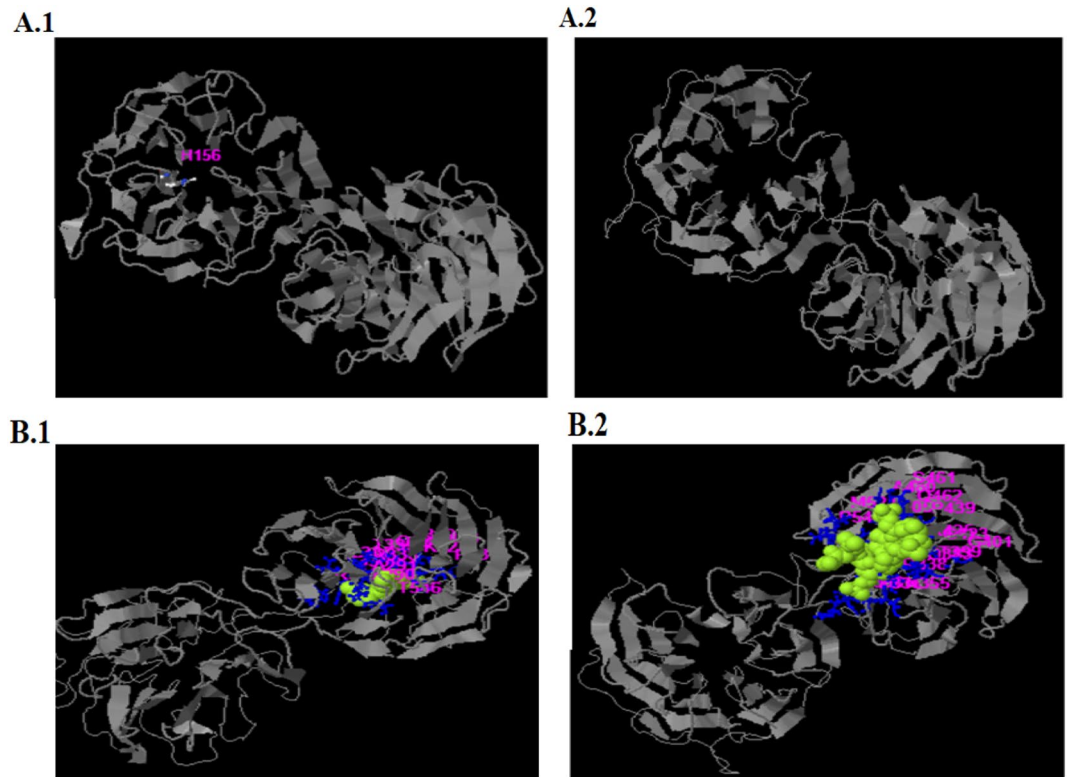


Figure 3. The overall effect of G352R variant on TLE6 structure, binding sites and active sites. **(A)** Comparison of mutant TLE6 binding sites with wild-type. (1. Wild-type/ 2. mutant). **(B)** Comparison of mutant TLE6 active sites with wild-type. (1. Wild-type/ 2. mutant).

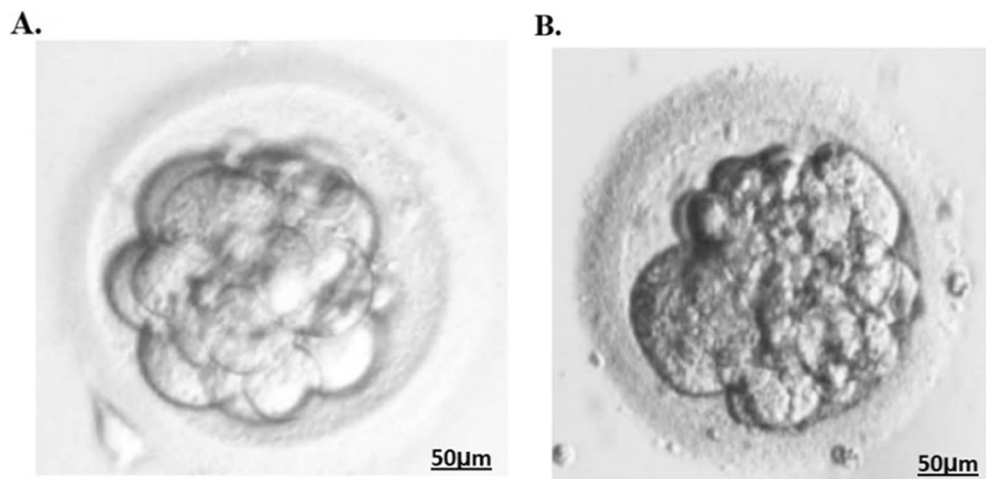


Figure 4. Phenotype of embryo from the proband (II-18).

TLE (Transducin-like enhancer protein) family is a conserved family of corepressor proteins, which cannot bind DNA directly but repress transcription by interacting with partner proteins^{33,42}. They repress gene expression through different mechanisms⁴³. Two evolutionarily conserved domains are found in the TLE family: the carboxy-terminal WD40 repeat domain and an amino-terminal (TLE N-terminal), also known as the Q-rich domain. It seems that the Q-rich domain is important for oligomerization of TLE and binding to specific transcription factors and interactions with most transcription factors are mediated by the WD40 repeat domain^{33,43,44}.

WD40-Repeat Proteins (WDR proteins) are one of the largest families encoded by humans⁷. They play important roles in many fundamental biological processes such as apoptosis⁸, DNA damage response¹⁷, protein degradation¹⁸, RNA processing¹⁸, transcription regulation^{20,21}, histone modification²², and signal transduction²³. WDR proteins often act as scaffolds to engage other molecules, forming protein–protein interactions or functional

complexes⁷. They are classified broadly into 21 classes based on their domain architectures⁷. Transducin-like enhancer protein (TLE) family belongs to Class 7 (TLE_N + WD40)^{7,24}.

There are four full-length *TLE* genes in humans named *TLE1-4* and three truncated forms, *TLE5-7*. The truncated *TLE* isoforms are thought to inhibit the function of the full-length TLEs (*TLE1-4*)³³. *TLE6* is located on chromosome 19 at 19p13.3. It contains 17 exons that span more than 17 kb of genomic DNA and it encodes the Transducin-like enhancer protein 6 (Q9H808-*TLE6*-Human) with 572 amino acids. Expressing in different tissue such as the placenta, thyroid, lung, and testis. It has 7 WDR domains.

To date, 13 variants have been identified in *TLE6*—associated with EDA characterized by female fertility^{34–40}. 64% of them were located in the WDR domain. This paper adds the 14th variant which is located in the WDR domain. The variant identified in this study (c.G1054C:p.G352R) leads to the replacement of Gly 352 with Arg residing in the buried residue of the WDR2 domain which plays a central role in enzyme activity. It is speculated that native *TLE6* has 3 Active site residues (156,125 and 145) and 33 ligand binding sites. This variant leads to missing all active sites and 20 native binding sites and also it leads to gaining 30 new binding sites.

By considering its roles in signaling pathways (Notch and Wnt)^{45,46} and some biological functions such as endoplasmic reticulum localization, spindle localization, mitochondrion localization, regulation of cell division, and regulation of transcription by RNA polymerase II, it would be clear that loss of its functions may lead to infertility.

In summary, this study extended the spectrum of genetic causes of familial female infertility characterized by EDA by reporting a novel variant in *TLE6*. Our result suggests oocyte donation as the best ART method for patients with biallelic *TLE6* variants right now.

Data availability

The datasets used and/or analyzed during the current study are available from the corresponding author on reasonable request. The identified variant in this study has been deposited into NCBI, ClinVar (accession number: SCV002525878) and will be publicly available per NCBI "Hold until publish" policy.

Received: 7 May 2022; Accepted: 18 October 2022

Published online: 21 October 2022

References

1. VC, R. R., Jogi, P., Bolem, O., Guju, E. & Sanaboina, A. A review on risk factors, staging and survival rates of endometrial cancer in both black and white women in infertility patients in USA. *World J. Curr. Med. Pharm. Res.* **2**, 152–156 (2020).
2. Morshed-Behbahani, B., Lamyian, M., Joulaei, H., Rashidi, B. H. & Montazeri, A. Infertility policy analysis: A comparative study of selected lower middle-middle-and high-income countries. *Glob. Health* **16**, 1–9 (2020).
3. Moghadam, A. D., Delpisheh, A. & Sayehmiri, K. The trend of infertility in Iran, an original review and meta-analysis. *Nursing Practice Today* **1**, 46–52 (2014).
4. Betts, D. & Madan, P. Permanent embryo arrest: Molecular and cellular concepts. *MHR Basic Sci. Reproduct. Med.* **14**, 445–453 (2008).
5. Byrne, A., Southgate, J., Brison, D. & Leese, H. Analysis of apoptosis in the preimplantation bovine embryo using TUNEL. *Reproduction* **117**, 97–105 (1999).
6. Hardy, K. Apoptosis in the human embryo. *Rev. Reprod.* **4**, 125–134 (1999).
7. Matwee, C., Betts, D. H. & King, W. A. Apoptosis in the early bovine embryo. *Zygote* **8**, 57–68 (2000).
8. Gjorret, J. O. *et al.* Chronology of apoptosis in bovine embryos produced in vivo and in vitro. *Biol. Reprod.* **69**, 1193–1200 (2003).
9. Mu, J. *et al.* Mutations in NLRP2 and NLRP5 cause female infertility characterised by early embryonic arrest. *J. Med. Genet.* **56**, 471–480 (2019).
10. Wang, W. *et al.* FBXO43 variants in patients with female infertility characterized by early embryonic arrest. *Hum. Reprod.* **36**, 2392–2402 (2021).
11. Wang, X. *et al.* A novel homozygous mutation in the PADI6 gene causes early embryo arrest. *Reprod. Health* **19**, 1–11 (2022).
12. Yu, C. *et al.* BTG4 is a meiotic cell cycle-coupled maternal-zygotic-transition licensing factor in oocytes. *Nat. Struct. Mol. Biol.* **23**, 387–394 (2016).
13. Zhao, L. *et al.* Biallelic mutations in CDC20 cause female infertility characterized by abnormalities in oocyte maturation and early embryonic development. *Protein Cell* **11**, 921–927 (2020).
14. Zhang, Y. L. *et al.* Biallelic mutations in MOS cause female infertility characterized by human early embryonic arrest and fragmentation. *EMBO Mol. Med.* **13**, e14887 (2021).
15. Zeng, Y. *et al.* Bi-allelic mutations in MOS cause female infertility characterized by preimplantation embryonic arrest. *Hum. Reprod.* **37**, 612–620 (2022).
16. Xin, A. *et al.* Disruption in ACTL7A causes acrosomal ultrastructural defects in human and mouse sperm as a novel male factor inducing early embryonic arrest. *Sci. Adv.* **6**, eaaz4796 (2020).
17. Mohebi, M. & Ghafouri-Fard, S. Embryo developmental arrest: Review of genetic factors and pathways. *Gene Rep.* **17**, 100479 (2019).
18. Wu, D. & Dean, J. Maternal factors regulating preimplantation development in mice. *Curr. Top. Dev. Biol.* **140**, 317–340 (2020).
19. Luong, X. G. & Conti, M. *Human Reproductive and Prenatal Genetics* 193–220 (Elsevier, 2019).
20. Feng, M., Bai, Y., Chen, Y. & Wang, K. Knockout of the Transducin-like enhancer of split 6 gene affects the proliferation and cell cycle process of mouse spermatogonia. *Int. J. Mol. Sci.* **21**, 5827 (2020).
21. Yu, X.-J. *et al.* The subcortical maternal complex controls symmetric division of mouse zygotes by regulating F-actin dynamics. *Nat. Commun.* **5**, 1–12 (2014).
22. Zhu, K. *et al.* Identification of a human subcortical maternal complex. *MHR Basic Sci. Reproduct. Med.* **21**, 320–329 (2015).
23. Bebbere, D., Albertini, D. F., Cotichio, G., Borini, A. & Ledda, S. The subcortical maternal complex: Emerging roles and novel perspectives. *Mol. Hum. Reproduct.* **27**, gaab043 (2021).
24. Zou, X.-D. *et al.* Genome-wide analysis of WD40 protein family in human. *Sci. Rep.* **6**, 1–11 (2016).
25. Zou, H., Henzel, W. J., Liu, X., Lutschg, A. & Wang, X. Apaf-1, a human protein homologous to *C. elegans* CED-4, participates in cytochrome c-dependent activation of caspase-3. *Cell* **90**, 405–413 (1997).
26. Wakasugi, M. *et al.* DDB accumulates at DNA damage sites immediately after UV irradiation and directly stimulates nucleotide excision repair. *J. Biol. Chem.* **277**, 1637–1640 (2002).

27. Higa, L. A. *et al.* CUL4–DDB1 ubiquitin ligase interacts with multiple WD40-repeat proteins and regulates histone methylation. *Nat. Cell Biol.* **8**, 1277–1283 (2006).
28. Yan, C. *et al.* Structure of a yeast spliceosome at 3.6-angstrom resolution. *Science* **349**, 1182–1191 (2015).
29. Jennings, B. H. *et al.* Molecular recognition of transcriptional repressor motifs by the WD domain of the Groucho/TLE corepressor. *Mol. Cell* **22**, 645–655 (2006).
30. Znaidi, S., Pelletier, B., Mukai, Y. & Labbé, S. The Schizosaccharomyces pombe corepressor Tup11 interacts with the iron-responsive transcription factor Fep1. *J. Biol. Chem.* **279**, 9462–9474 (2004).
31. Ruthenburg, A. J. *et al.* Histone H3 recognition and presentation by the WDR5 module of the MLL1 complex. *Nat. Struct. Mol. Biol.* **13**, 704–712 (2006).
32. Gaudet, R., Bohm, A. & Sigler, P. B. Crystal structure at 2.4 Å resolution of the complex of transducin β and its regulator, phosphodiesterase-3. *Cell* **87**, 577–588 (1996).
33. Agarwal, M., Kumar, P. & Mathew, S. J. The Groucho/Transducin-like enhancer of split protein family in animal development. *IUBMB Life* **67**, 472–481 (2015).
34. Mao, B. *et al.* A novel TLE6 mutation, c. 541 + 1G> A, identified using whole-exome sequencing in a Chinese family with female infertility. *Mol. Genet. Genom. Med.* **9**, e1743 (2021).
35. Liu, J. *et al.* Two novel mutations in PADI6 and TLE6 genes cause female infertility due to arrest in embryonic development. *J. Assist. Reprod. Genet.* **38**, 1551–1559 (2021).
36. Wang, L.-Q. *et al.* LncRNA-Fendrr protects against the ubiquitination and degradation of NLRC4 protein through HERC2 to regulate the pyroptosis of microglia. *Mol. Med.* **27**, 39. <https://doi.org/10.1186/s10020-021-00299-y> (2021).
37. Zheng, W. *et al.* Expanding the genetic and phenotypic spectrum of the subcortical maternal complex genes in recurrent preimplantation embryonic arrest. *Clin. Genet.* **99**, 286–291 (2021).
38. Lin, J. *et al.* Expanding the genetic and phenotypic spectrum of female infertility caused by TLE6 mutations. *J. Assist. Reprod. Genet.* **37**, 437–442 (2020).
39. Wang, X. *et al.* Novel mutations in genes encoding subcortical maternal complex proteins may cause human embryonic developmental arrest. *Reprod. Biomed. Online* **36**, 698–704 (2018).
40. Alazami, A. M. *et al.* TLE6 mutation causes the earliest known human embryonic lethality. *Genome Biol.* **16**, 1–8 (2015).
41. Zhang, M. *et al.* Identification of novel biallelic TLE6 variants in female infertility with preimplantation embryonic lethality. *Front. Genet.* **894** (2021).
42. Beagle, B. & Johnson, G. V. AES/GRG5: More than just a dominant-negative TLE/GRG family member. *Dev. Dyn.* **239**, 2795–2805 (2010).
43. Turki-Judeh, W. & Courey, A. J. Groucho: A corepressor with instructive roles in development. *Curr. Top. Dev. Biol.* **98**, 65–96 (2012).
44. Jennings, B. H. & Ish-Horowicz, D. The Groucho/TLE/Grp family of transcriptional co-repressors. *Genome Biol.* **9**, 1–7 (2008).
45. Salazar, J. L. & Yamamoto, S. Integration of Drosophila and human genetics to understand notch signaling related diseases. *Mol. Mech. Notch Signaling*. **1066**, 141–185 (2018).
46. Tribulo, P. *et al.* WNT regulation of embryonic development likely involves pathways independent of nuclear CTNBN1. *Reproduction* **153**, 405–419 (2017).

Acknowledgements

This study was financially supported by both Shahid Beheshti University of Medical Sciences and Tehran University of Medical Sciences.

Author contributions

Conceptualization: S.G.F., M.H.M., M.A., M.M., K.B. Data curation: M.A., A.G. Formal analysis: M.A., M.H.M., K.B. Methodology: M.A., A.G. Visualization: M.A., M.H.M., K.B. Writing original draft: M.A., M.M. Writing review and editing: M.A., M.M., and S.G.F. Supervision: S.G.F., M.H.M.

Competing interests

The authors declare no competing interests.

Additional information

Correspondence and requests for materials should be addressed to M.H.M. or S.G.-F.

Reprints and permissions information is available at www.nature.com/reprints.

Publisher's note Springer Nature remains neutral with regard to jurisdictional claims in published maps and institutional affiliations.



Open Access This article is licensed under a Creative Commons Attribution 4.0 International License, which permits use, sharing, adaptation, distribution and reproduction in any medium or format, as long as you give appropriate credit to the original author(s) and the source, provide a link to the Creative Commons licence, and indicate if changes were made. The images or other third party material in this article are included in the article's Creative Commons licence, unless indicated otherwise in a credit line to the material. If material is not included in the article's Creative Commons licence and your intended use is not permitted by statutory regulation or exceeds the permitted use, you will need to obtain permission directly from the copyright holder. To view a copy of this licence, visit <http://creativecommons.org/licenses/by/4.0/>.

© The Author(s) 2022, corrected publication 2022